Surface direct nuclear photoeffect in heavy deformed nuclei

B. S. Ishkhanov,[1,2] V. N. Orlin,[2] and K. A. Stopani[2]
[1]*Lomonosov Moscow State University, Department of Physics, Moscow 119991, Russia*
[2]*Lomonosov Moscow State University, Skobeltsyn Institute of Nuclear Physics, Moscow 119991, Russia*
(Received 13 July 2016; published 30 November 2016)

A mechanism of photon-induced direct knockout of a nucleon from the nuclear surface without formation of intermediate excited nuclear state is described. The effect plays an important role at least for the (γ, p) reaction on heavy nuclei in the energy region centered at about 30 MeV where the probability of formation of the giant dipole resonance is already small but quasideuteron photoabsorption still does not prevail. A compact model of the surface direct nuclear photoeffect (SDNP) in heavy deformed nuclei that can be used to calculate the differential $d\sigma(E_\gamma, \vartheta)/d\Omega$ and total $\sigma(E_\gamma)$ cross sections of the SDNP under adiabatic approximation is formulated. The model is applied to calculation of the (γ, p) reaction cross sections on ^{160}Gd and ^{184,186}W. The importance of the SDNP effect for these nuclei at $E_\gamma \sim 30$ MeV is demonstrated.

DOI: 10.1103/PhysRevC.94.054623

I. INTRODUCTION

Description of the nuclear photoeffect, i.e., emission of nucleons in photonuclear reactions, is typically performed within semiclassical [1–7] or quantum multistep [8–14] pre-equilibrium models in combination with the Weisskopf-Ewing or Hauser-Feshbach statistical models. Such models treat an excited nucleus as a composite system approaching to statistical equilibrium, and successfully describe emission of photoneutrons over a wide range of mass numbers A and incident photon energies E_γ (up to the π meson production threshold). However, these models are not able to explain the experimentally observable excess yield of photoprotons from nuclei with $A > 100$ at the high-energy tail of the giant dipole resonance (GDR), which indicates a significant contribution to the (γ, p) reaction, in this case from the direct mechanism nuclear photoeffect [15].

In the late 1950s, a description of the direct nuclear photoeffect based on the shell model was proposed in a series of works [16–18]. It was assumed that direct photonucleons are emitted directly from the doorway $(1p1h)$ configurations that are excited during absorption of a $E1$ photon. The energies of such configurations had been shifted towards higher energies so as to align the computed excitation energy with the actual position of the GDR. Under these assumptions it follows (1) that the direct photonucleon yield is at maximum near the peak of the GDR and gradually decreases at higher energies matching its behavior, and (2) that the angular distribution of the emitted nucleons is not isotropic, with increased probability of emission at 90° to the direction of motion of the absorbed photon. In fact, this model describes the semidirect nuclear photoeffect, since the GDR excitation is involved in the nucleon knockout process. Apparently, this model as well as the statistical approach cannot explain the large yield of photoprotons in heavy nuclei at the high-energy tail of the GDR.

Therefore, at large energies E_γ a major contribution to the (γ, p) reaction arises not only from the semidirect photoeffect, but also from direct nucleon knockout from single-particle bound states of the target nucleus. In Ref. [15] the high-energy bump corresponding to the protons emitted from the ^{197}Au(γ, p) reaction was interpreted in terms of the direct-semidirect (DSD) model developed in [19–22]. In the DSD model, one explicitly considers only the first stage of the reaction that includes both the direct process of nucleon knockout (capture) and nucleon emission (absorption) with excitation of a multipole giant resonance. Interaction of the direct and semidirect reaction mechanisms as well as the effects of more complex processes are taken into account through modification of the multipole operators and form factors describing decay and excitation of the multipole giant resonances. Presently, the DSD model formalism allows calculations only for nuclei with closed or almost closed single-particle subshells.

It is unlikely that the excess yield of photoprotons from heavy nuclei above the giant dipole resonance (about 30 MeV) can be explained as direct knockout of nucleons from deep-lying subshells of the target nucleus, since the probability of this process is low compared to the probability of the competing process of excitation of a composite state with subsequent emission of semidirect and statistical nucleons. Therefore, one is left to presume that the considered effect is a result of the knockout of a nucleon from the surface layer of the target nucleus (from the outermost subshell), when the absorbed photon energy is almost entirely spent to the knockout of a bound nucleon which then moves in the average field while the core of the target nucleus only experiences recoil. This process, which is called the surface direct nuclear photoeffect (SDNP) in the rest of the present work, is illustrated in Fig. 1.

The overall contribution of the described effect should not be, at first glance, very considerable. However, it follows from simple semiclassical argumentation that there can be cases where it results in a significant yield of photoprotons. As it is seen from Fig. 1, when a nucleon is knocked out from the peripheral region of a nucleus due to photon absorption the nucleus receives an orbital momentum $l \approx k_\gamma R$, where $k_\gamma = E_\gamma/\hbar c$ fm^{-1} is the wave vector transfer and $R = 1.2A^{1/3}$ fm is the radius of the nucleus. Since l can take only integer values in quantum mechanics, it is natural to expect that when l is approximately an integer a maximum appears in the SDNP

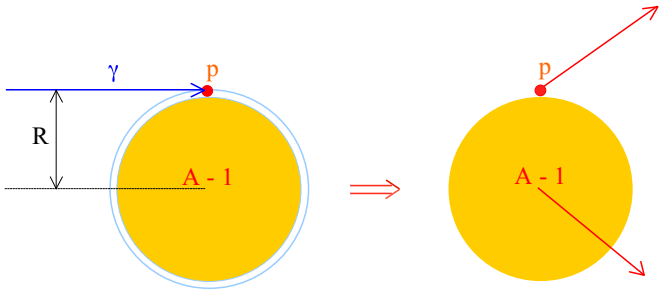

FIG. 1. Schematic illustration of the proton surface direct photoeffect.

cross section. The lowest lying "resonance" is expected at $l = 1$, which corresponds to electric dipole absorption and is placed at the energy of about $E_\gamma \sim 165A^{-1/3}$ MeV. Thus, the SDNP yield should be expected to be noticeable for heavy nuclei with $A \sim 150$–200 in the $E_\gamma \sim 30$-MeV region.

The SDNP amplitude corresponding to the knockout of a nucleon from a single-particle level jm can be approximated by the product $\langle f|a(jm)|0\rangle\langle \mathbf{k}^{(-)}|H_{\rm ptb}|jm\rangle$, where the first term is the matrix element of the $a(jm)$ annihilation operator corresponding to a transition from the ground state $|0\rangle$ of the initial nucleus to the $|f\rangle$ state (ground state or a low-lying excitation) of the final nucleus (coefficient of fractional parentage), and the second term describes a photon-induced transition of a single nucleon from the jm orbital to the stationary scattering state $|\mathbf{k}^{(-)}\rangle$ in the average field of the final nucleus with ingoing waves, corresponding to the emission of a nucleon with the wave vector $\mathbf{k}$.

Calculation SDNP in spherical nuclei is complicated by the fact that due to the effect of the residual interaction the actual wave functions of the $|0\rangle$ and $|f\rangle$ states for open-shell nuclei can be very different from the simple multiparticle shell wave functions. An exception is comprised by magic or sufficiently close to magic nuclei and light nuclei with closed subshells where the SDNP can be calculated using the direct knockout model developed in [23–25]. In this model, it is assumed (1) that the states of the initial and final nuclei can be described using a independent-particle shell model, (2) that the photon is absorbed by a single bound nucleon that is subsequently emitted into continuum, while other nucleons form an inert core. If the final nucleus is produced in the ground state it is easily seen that this reaction mechanism corresponds to the SDNP. The direct process contribution to cross sections of the reactions ^{12}C$(\gamma,p_0)^{11}$B, ^{12}C$(\gamma,n_0)^{11}$C, ^{16}O$(\gamma,p_0)^{15}$N, and ^{40}Ca$(\gamma,p_0)^{39}$K was calculated in [23–25].

The complexity of SDNP computation is also significantly reduced in the case of heavy axially symmetric deformed nuclei with sufficiently hard surface, for which the ground state wave function in the intrinsic frame can be approximated as an antisymmetrized product of single-particle (or quasiparticle) states of nucleons in filled orbitals of a deformed nuclear potential, which allows a general solution to the formulated problem to be obtained. In this work we limit ourselves to consideration of SDNP only in such nuclei.

The present work is structured as follows. The basic assumptions used for description of the SDNP in deformed nuclei with general expressions for the differential $\frac{d\sigma}{d\Omega}(E_\gamma,\vartheta)$ and total $\sigma(E_\gamma)$ cross sections under adiabatic approximation are formulated in Sec. II. In Sec. III a system of algebraic equations for the coupled lj reaction channels used for calculation of the scattering state of nucleon at $r \lesssim R_{\rm peak} \approx 1.6A^{1/3}$ fm in the deformed average nuclear field is described. Section IV contains a description of the procedure used to replace the spherically symmetric optical potential by a deformed optical potential as an approximation of the average nuclear field in which motion of the outgoing nucleon takes place. Thus, a complete model of the SDNP for deformed nuclei is constructed, after which in Sec. V it is applied to the (γ,p) reactions in ^{160}Gd and ^{184,186}W. In the Conclusions section the main results of the present work are summarized and characteristic properties of the SDNP that can be used to distinguish this process from other nuclear photoeffect mechanisms are outlined.

II. ADIABATIC APPROXIMATION

The description of the surface direct nuclear photoeffect in this work is based on the following assumptions:

(1) the consideration is limited only to heavy, axially symmetric deformed nuclei;
(2) the adiabatic condition is met: the velocity of rotational motion of the deformed nucleus and, thus, of the average nuclear field, is negligible in comparison with the velocity of the outgoing nucleon knocked out by the photon, so its motion is not disturbed by the rotation;
(3) the photon interacts only with one of the nucleons from the last-filled orbital of the initial nucleus, other nucleons remain in their initial orbitals, and the final nucleus remains in the ground state in intrinsic coordinate frame;
(4) the initial electromagnetic interaction of the photon with the target nucleus is considered within the time-dependent perturbation theory under the assumption that the main contribution to the reaction corresponds to electric dipole absorption, according to the semiclassical argumentation in the Introduction;
(5) the average nuclear field that interacts with the outgoing nucleon is approximated with a deformed optical potential (its construction is described below).

Under these assumptions the differential cross section of nucleon emission due to SDNP in the intrinsic frame $\{x',y',z'\}$, the z' axis of which is directed along the symmetry axis of the nucleus, can be represented as

$$\frac{d\sigma_{\rm int}(E_\gamma,\vartheta',\phi')}{d\Omega'} = \frac{4}{3}\pi^3\frac{mkE_\gamma e_{\rm eff}^2}{c\hbar^3}\frac{1}{2} \times \sum_{\mu=\pm1}\sum_{s=\pm\frac{1}{2}}\left|\sum_\nu D^1_{\mu\nu}(\omega)\langle\langle(\mathbf{k}s)^{(-)}|r'Y_{1\nu}(\theta',\varphi')|\beta\rangle\right|^2, \quad (1)$$

where m is the reduced mass of the nucleon, $e_{\rm eff}$ is the effective nucleon charge (equal to eN/A for a proton, and $-eZ/A$ for a neutron; Eq. 3C-35 in [26]), $|(\mathbf{k}s)^{(-)}\rangle\rangle$[1] is the scattering state in the average field of the deformed final nucleus with ingoing spherical waves, that corresponds to an outgoing nucleon with the wave vector $\mathbf{k}$ and projection of spin onto the z' axis $s=\pm\frac{1}{2}$, $k=|\mathbf{k}|=\sqrt{2m\varepsilon}/\hbar$ is the absolute value of the wave vector of the outgoing nucleon, $\varepsilon=E_\gamma-B_{\rm thr}$ is its energy ($B_{\rm thr}$ is the nucleon separation energy of the target nucleus), ϑ',ϕ' are the polar and azimuthal angles of the emitted nucleon in intrinsic frame, $|\beta\rangle$ is the initial single particle state from which the nucleon is knocked out (since the target nucleus is axially symmetric it has a defined value m_β of the angular momentum projection onto the symmetry axis z'), $D^1_{\mu\nu}(\omega)$ is the finite rotation matrix describing transformation of the electric dipole moment operator from the intrinsic $\{x',y',z'\}$ to the laboratory $\{x,y,z\}$ frame, where the z axis coincides with the direction of motion of the incident photon, $\omega\equiv\{\theta_1,\theta_2,\theta_3\}$ are the Euler angles defining the position of the intrinsic frame relative to the laboratory frame, and the $\mu=\pm\frac{1}{2}$ quantum number accounts for two possible circular polarization states of the photon. Thus, the summation in (1) takes into account different spin orientations of the outgoing nucleon and averaging over photon polarization states.

In the case of an even number of nucleons in the last-filled orbital one of the two nucleons with $j_{z'}=\pm m_\beta$ is knocked out by the photon with equal probabilities. Without the nuclear pairing effect this should imply a twofold increase of cross section (1). However, due to pairing the probability that the nucleon pair is in the state ν close to the Fermi surface is less than 1. In deformed nuclei this probability can be approximated by the following expression [27]:

$$v_\nu^2=\frac{1}{2}\left[1-\frac{\varepsilon_\nu-\lambda}{\sqrt{(\varepsilon_\nu-\lambda)^2-\Delta_\nu^2}}\right], \tag{2}$$

where ε_ν is the energy of the single-particle state ν, λ is the chemical potential, and Δ_ν is the pairing energy. Since λ is approximately equal to the energy of the last-filled orbital $|\beta\rangle$, then an approximate relationship is obtained $v_\beta^2\approx\frac{1}{2}$ and no additional coefficient is required in (1).

The $|(\mathbf{k}s)^{(-)}\rangle\rangle$ state can be expanded into spherical harmonics:

$$|(\mathbf{k}s)^{(-)}\rangle\rangle=\frac{\hbar}{\sqrt{mk}}\sum_{l=0}^{\infty}\sum_{j=|l-1/2|}^{l+1/2}\sum_{m=-j}^{j}\left(l,m-s,\frac{1}{2},s|jm\right)\times Y^*_{lm-s}(\theta',\phi')|\alpha^{(-)}\rangle\rangle, \tag{3}$$

where $|\alpha^{(-)}\rangle\rangle\equiv|(\varepsilon ljm)^{(-)}\rangle\rangle$ are the scattering states in the average nuclear field with the energy $\varepsilon=\frac{\hbar^2k^2}{2m}$, which are not eigenstates of $\mathbf{l}^2$ and $\mathbf{j}^2$ operators in the case of deformed field (and do not have corresponding definite quantum numbers l and j), but still have the special property that a wave packet

$$\int_{-\infty}^{\infty}\frac{\gamma/\pi}{(\varepsilon-\varepsilon_0)^2+\gamma^2}e^{-i\varepsilon t}|\alpha^{(-)}\rangle\rangle\,d\varepsilon$$

built from them approaches at $t\to+\infty$ the wave packet

$$\int_{-\infty}^{\infty}\frac{\gamma/\pi}{(\varepsilon-\varepsilon_0)^2+\gamma^2}e^{-i\varepsilon t}|\varepsilon ljm\rangle\rangle_{\rm free}\,d\varepsilon$$

of freely moving nucleons with fixed l, j. With spheroidally deformed field the $|\alpha^{(-)}\rangle\rangle$ states have also a definite parity π and projection m of the angular moment $\mathbf{j}$ onto the nuclear symmetry axis. The $\frac{\hbar}{\sqrt{mk}}$ factor accounts for the difference in the normalization of the $|(\mathbf{k}s)^{(-)}\rangle\rangle$ and $|(\alpha^{(-)}\rangle\rangle$ states:

$$\langle\langle(\mathbf{k}'s')^{(-)}|(\mathbf{k}s)^{(-)}\rangle\rangle=\delta(\mathbf{k}'-\mathbf{k})\,\delta_{s's}, \tag{4}$$

$$\langle\langle\alpha'^{(-)}|\alpha^{(-)}\rangle\rangle=\delta_{\alpha'\alpha}\equiv\delta(\varepsilon'-\varepsilon)\delta_{l'l}\delta_{j'j}\delta_{m'm}. \tag{5}$$

Substituting expansion (3) into (1) and summing over s yields

$$\begin{aligned}\frac{d\sigma_{\rm intr}(E_\gamma,\vartheta')}{d\Omega'}&=\frac{\pi^2}{6}\frac{E_\gamma e_{\rm eff}^2}{c\hbar}\sum_{\mu=\pm1}\sum_{\nu}\sum_{\nu'}\sum_{ljm}\sum_{l'j'}\sum_{l''}D^1_{\mu\nu}(\omega)D^{1*}_{\mu\nu'}(\omega)\\&\times P_{l''}(\cos\vartheta')(-1)^{j+j'+\frac{1}{2}-m+l''}\,\hat{j}\,\hat{j}'\,\hat{l}\,\hat{l}'\,\hat{l}''^2\\&\times\begin{pmatrix}l&l'&l''\\0&0&0\end{pmatrix}\begin{pmatrix}j&l&j'\\-m&0&m\end{pmatrix}\begin{Bmatrix}j&l''&j'\\l'&\frac{1}{2}&l\end{Bmatrix}\\&\times\langle\langle\alpha^{(-)}|r'Y_{1\nu}(\theta',\varphi')|\beta\rangle\langle\langle\alpha'^{(-)}|r'Y_{1\nu'}(\theta',\varphi')|\beta\rangle^*\Big|_{\varepsilon'=\varepsilon},\end{aligned} \tag{6}$$

where the notation $\hat{J}=\sqrt{2J+1}$ is used.

Formula (6) describes angular distributions of photonucleons in the intrinsic coordinate frame whose fixed position relative to the laboratory frame is determined by the Euler angles ω. In order to obtain angular distribution of photonucleons (under adiabatic approximation) in the laboratory frame one has to do the following:

(1) transform the components of the spherical tensor $P_{l''}(\cos\vartheta')=\sqrt{\frac{4\pi}{2l''+1}}Y_{l''0}(\vartheta',\phi')$ in (6) to the laboratory frame:

$$Y_{l''0}(\vartheta',\phi')=\sum_{m''}D^{l''*}_{m''0}(\omega)Y_{l''m''}(\vartheta,\phi); \tag{7}$$

(2) perform averaging of the obtained expression over all possible orientations of the nucleus in the laboratory frame, which effectively reduces to computation of the integral $\frac{1}{8\pi^2}\int_0^\pi\sin\theta_1d\theta_1\int_0^{2\pi}d\theta_2\int_0^{2\pi}d\theta_3D^1_{\mu\nu}(\omega)D^{1*}_{\mu\nu'}(\omega)D^{l''*}_{m''0}(\omega)$,

(3) after which summation over the quantum numbers μ, ν', and m'' has to be performed.

As a result the following expression for the differential cross section of SDNP in laboratory frame is obtained:

$$\frac{d\sigma(E_\gamma,\vartheta)}{d\Omega}=\frac{\pi^2}{6}\frac{E_\gamma e_{\rm eff}^2}{c\hbar}\{A_0+A_2P_2(\cos\vartheta)\}, \tag{8}$$

[1]Throughout the text the scattering states in the deformed average field are denoted using the $|\ldots\rangle\rangle$ symbol, while scattering states in spherical average field use the $|\ldots\rangle$ notation.

where

$$A_0 = \frac{2}{3}\sum_{lj}\sum_{\nu m}|\langle\langle\alpha^{(-)}|r'Y_{1\nu}(\theta',\varphi')|\beta\rangle|^2, \quad (9)$$

$$A_2 = -\sqrt{\frac{10}{3}}\sum_{lj}\sum_{l'j'}\sum_{\nu m}(-1)^{j+j'+1/2-m+\nu}\,\hat{j}\,\hat{j}'\,\hat{l}\,\hat{l}' \times \begin{pmatrix} l & l' & 2 \\ 0 & 0 & 0 \end{pmatrix}\begin{pmatrix} j & 2 & j' \\ -m & 0 & m \end{pmatrix}\begin{Bmatrix} j & 2 & j' \\ l' & \frac{1}{2} & l \end{Bmatrix} \times \begin{pmatrix} 1 & 1 & 2 \\ -\nu & \nu & 0 \end{pmatrix}\langle\langle\alpha^{(-)}|r'Y_{1\nu}(\theta',\varphi')|\beta\rangle \times \langle\langle\alpha'^{(-)}|r'Y_{1\nu}(\theta',\varphi')|\beta\rangle^*\Big|_{\varepsilon'=\varepsilon,m'=m}. \quad (10)$$

As expected the angular distribution of direct photonucleons associated with $E1$ photon absorption is symmetric with respect to the $\vartheta = 90^\circ$ angle between the directions of motion of the outgoing nucleon and the incident photon.

Integration of Eq. (8) over the polar ϑ and azimuthal ϕ angles of the outgoing nucleon yields the total cross section of SDNP in the considered approximation:

$$\sigma(E_\gamma) = \frac{4\pi^3}{9}\frac{E_\gamma e^2_{\rm eff}}{c\hbar}\sum_{lj}\sum_{\nu m}|\langle\langle\alpha^{(-)}|r'Y_{1\nu}(\theta',\varphi')|\beta\rangle|^2. \quad (11)$$

At the end of this section it should be emphasized that computation of all matrix elements in (9)–(11) is performed in the intrinsic coordinate frame $\{x',y',z'\}$.

III. SYSTEM OF EQUATIONS DESCRIBING COUPLED lj REACTION CHANNELS

As it was mentioned above, an axially symmetric deformed optical potential $V(r,\theta)$ will be used for description of the average field in which motion of the outgoing nucleon takes place (in the following, the prime marks at spatial variables in intrinsic coordinate frame will be omitted). The potential can be split into two parts:

$$V(r,\theta) = V_{\rm sph}(r) + V_{\rm def}(r,\theta), \quad (12)$$

where $V_{\rm sph}(r)$ is a usual spherical optical potential (see [28]) and $V_{\rm def}(r,\theta)$ is the part of the optical potential depending on the polar angle θ, which leads to coupling between the reaction channels for scattering states with different values of the angular momentum l,j.

As shown in [29] the scattering state $|(\mathbf{k}s)^{(-)}\rangle\rangle$ in potential (12) can be expressed in the form

$$|(\mathbf{k}s)^{(-)}\rangle\rangle = |(\mathbf{k}s)^{(-)}\rangle + \frac{1}{\varepsilon - H - i\rho}V_{\rm def}|(\mathbf{k}s)^{(-)}\rangle, \quad \rho\to+0, \quad (13)$$

where $H = H_{\rm sph} + V_{\rm def}$ is the total single-particle Hamiltonian of the system, $H_{\rm sph} = \frac{-\hbar^2}{2m}\Delta + V_{\rm sph}$ is its spherical component, $|(\mathbf{k}s)^{(-)}\rangle$ is the scattering state with ingoing waves corresponding to $H_{\rm sph}$.

An important property of (13) is fulfillment of proper boundary conditions for the scattering state $|(\mathbf{k}s)^{(-)}\rangle\rangle$. Using expansion (3) it can be transformed into an equation for partial waves $|\alpha^{(-)}\rangle\rangle$:

$$|\alpha^{(-)}\rangle\rangle = |\alpha^{(-)}\rangle + \frac{1}{\varepsilon - H - i\rho}V_{\rm def}|\alpha^{(-)}\rangle. \quad (14)$$

Here, $|\alpha^{(-)}\rangle \equiv |(\varepsilon ljm)^{(-)}\rangle$ is the nucleon scattering with ingoing waves in the spherical average field $V_{\rm sph}$, that is characterized by the nucleon energy ε, its orbital and total angular momentum values l and j, and the angular momentum projection m.

Matrix elements $\langle\langle\alpha^{(-)}|rY_{1\nu}(\theta,\varphi)|\beta\rangle$ that appear in the SDNP cross sections $\frac{d\sigma}{d\Omega}(E_\gamma,\vartheta)$ and $\sigma(E_\gamma)$ [Eqs. (8)–(11)] describe the amplitudes of $E1$ transition of the nucleon from the bound state $|\beta\rangle$ to the scattering state $|\alpha^{(-)}\rangle\rangle$. This implies that the conjugate states (Dirac's bra-vectors) $\langle\langle\alpha^{(-)}|$ in the continuous spectrum and $\langle n|$ in the discrete spectrum have to be orthogonal to the eigenstates $|\alpha^{(-)}\rangle\rangle$ and $|n\rangle$ of the Hamiltonian H.

In our case the Hamiltonian contains the complex optical potential and is, therefore, non-Hermitian. In order to construct such states we note that the states $\langle\Psi_1|,\langle\Psi_2|,\ldots,$ that are conjugate to the eigenvectors $|\Psi_1\rangle,|\Psi_2\rangle,\ldots$ of some non-Hermitian Hamiltonian $\tilde{H} \neq \tilde{H}^+ = \tilde{H}^*$, will meet the necessary requirements if they are defined via the following equations:

$$\langle\Psi_i|\tilde{H} = E_i\langle\Psi_i|, \quad i = 1,2,\ldots. \quad (15)$$

Indeed, in this case $\langle\Psi_i|\tilde{H}|\Psi_k\rangle = E_i\langle\Psi_i|\Psi_k\rangle = E_k\langle\Psi_i|\Psi_k\rangle$. It follows that $\langle\Psi_i|\Psi_k\rangle = 0$ when $E_i \neq E_k$.

Equation (15) can be rewritten as (with ξ being the spin variable)

$$\sum_{\xi=\pm\frac{1}{2}}\int\langle\mathbf{r}'\xi'|\tilde{H}^*|\mathbf{r}\xi\rangle\langle\Psi_i|\mathbf{r}\xi\rangle^* d^3r = E_i^*\langle\Psi_i|\mathbf{r}'\xi'\rangle^*, \quad (16)$$

from which it follows that (up to the phase factor $e^{i\varphi_i}$) when $\tilde{H}^* \neq \tilde{H}$ the wave function $\langle\Psi_i|\mathbf{r}\xi\rangle$ of the conjugate state $\langle\Psi_i|$ is a complex conjugate to the wave function of the eigenstate of $\tilde{H}^*$, and not $\tilde{H}$. The phase factors can always be chosen is such a way that the orthonormality and completeness conditions of the states $\{|\Psi_i\rangle\}$ have the usual form:

$$\langle\Psi_i|\Psi_k\rangle = \delta_{ik}, \quad (17)$$

$$\sum_i|\Psi_i\rangle\langle\Psi_i| = 1. \quad (18)$$

In this way we obtain an equation for the conjugate scattering state $\langle\langle\alpha^{(-)}|$. Taking into account the decomposition of the Hamiltonian H into two parts from (15) we find

$$\langle\alpha^{(-)}|(H-\varepsilon) = \langle\alpha^{(-)}|V_{\rm def}.$$

It follows that the conjugate state $\langle\langle\alpha^{(-)}|$ that satisfies the equation $\langle\langle\alpha^{(-)}|(H-\varepsilon) = 0$ can be expressed in the form

$$\langle\langle\alpha^{(-)}| = \langle\alpha^{(-)}| + \langle\alpha^{(-)}|\,V_{\rm def}\frac{1}{\varepsilon - H + i\rho}, \quad (19)$$

where the sign in front of an infinitesimal constant ρ is chosen so as to ensure orthonormality of the scattering states, as shown

below: from (14) and (19) we have

$$\langle\langle\alpha'^{(-)}|\alpha^{(-)}\rangle\rangle = \delta_{\alpha'\alpha} + \frac{\langle\alpha'^{(-)}|V_{\rm def}|\alpha^{(-)}\rangle\rangle}{\varepsilon' - \varepsilon + i\rho} + \langle\alpha'^{(-)}|\frac{1}{\varepsilon - H - i\rho}V_{\rm def}|\alpha^{(-)}\rangle.$$

Then, using the identity

$$\langle\alpha'^{(-)}|\frac{1}{\varepsilon - H - i\rho} = \frac{1}{\varepsilon - \varepsilon' - i\rho}\left\{\langle\alpha'^{(-)}| + \langle\alpha'^{(-)}|V_{\rm def}\frac{1}{\varepsilon - H - i\rho}\right\}$$

and once again (14) we obtain

$$\langle\langle\alpha'^{(-)}|\alpha^{(-)}\rangle\rangle = \delta_{\alpha'\alpha} + \frac{1}{\varepsilon - \varepsilon' - i\rho}\{-\langle\alpha'^{(-)}|V_{\rm def}|\alpha^{(-)}\rangle\rangle + \langle\alpha'^{(-)}|V_{\rm def}|\alpha^{(-)}\rangle + \langle\alpha'^{(-)}|V_{\rm def}|\alpha^{(-)}\rangle\rangle - \langle\alpha'^{(-)}|V_{\rm def}|\alpha^{(-)}\rangle\} = \delta_{\alpha'\alpha}.$$

Which proves the statement.

The wave function of the scattering state $\langle\langle\alpha^{(-)}|$ overlaps with the wave function of the bound state $|\beta\rangle$ only in the internal reaction region (when $r \lesssim R_{\rm react} \approx 1.6A^{1/3}$ fm). In this limited space region the spherical harmonic oscillator states $|Nljm\rangle$ can be used as a basis (N denotes the total number of harmonic oscillator quanta). The $\langle\langle\alpha^{(-)}|rY_{1\nu}(\theta,\varphi)|\beta\rangle$ matrix element can, therefore, be expressed as

$$\langle\langle\alpha^{(-)}|rY_{1\nu}(\theta,\varphi)|\beta\rangle = \sum_{N'l'j'}\langle\langle\alpha^{(-)}|N'l'j'm\rangle\langle N'l'j'm|rY_{1\nu}(\theta,\varphi)|\beta\rangle, \quad (20)$$

where it is taken into account that in an axially symmetric field the scattering state has a definite value of the magnetic quantum number m.

The $\hbar\omega$ energy of the spherical oscillator is reasonable to be chosen so as to reproduce the experimental mean-squared radius of the nucleon distribution inside the nucleus. This yields the value $\hbar\omega = 41A^{-1/3}$ MeV.

The initial state of the nucleon $|\beta\rangle$ from which it is knocked out can also be approximated using the oscillator states $|Nljm\rangle$. Within the Nilsson deformed oscillator potential model [30,31] it will be of the form

$$|\beta\rangle = \sum_{lj\in\beta} c_{lj}\,|N_\beta\, ljm_\beta\rangle, \quad (21)$$

where c_{lj} are the coefficients of expansion of the state $|\beta\rangle$ into spherical oscillator states defined by the Nilsson model.

By substituting (21) into the matrix element $\langle N'l'j'm|rY_{1\nu}(\theta,\varphi)|\beta\rangle$, we obtain

$$\langle N'l'j'm|rY_{1\nu}(\theta,\varphi)|\beta\rangle = \sum_{lj\in\beta} c_{lj}\langle N'l'|r|N_\beta l\rangle\langle l'j'm|Y_{1\nu}(\theta,\varphi)|ljm_\beta\rangle, \quad (22)$$

where the radial matrix element $\langle N'l'|r|N_\beta l\rangle$ can be calculated using the analytical expression given in [30], and the angular matrix element $\langle l'j'm|Y_{1\nu}(\theta,\varphi)|ljm_\beta\rangle$ is determined by the relationship

$$\langle l_2 j_2 m_2|Y_{l\nu}(\theta,\varphi)|l_1 j_1 m_1\rangle = (-1)^{m_2-\frac{1}{2}}\sqrt{\frac{1}{4\pi}}\,\hat{l}_2\hat{l}_1\hat{j}_2\hat{j}_1\hat{l}\begin{pmatrix} l_2 & l & l_1\\ 0 & 0 & 0\end{pmatrix}\times\begin{pmatrix} j_2 & l & j_1\\ m_2 & -\nu & -m1\end{pmatrix}\begin{Bmatrix} j_2 & l & j_1\\ l_1 & \frac{1}{2} & l_2\end{Bmatrix}. \quad (23)$$

The task of calculation of the amplitudes (20) is, therefore, reduced to calculation of the $Nljm$ components of the conjugate scattering states $\langle\langle\alpha^{(-)}|$ in the internal region of the reaction.

In order to obtain the system of equations connecting these components and, consequently, different lj scattering channels we reformulate expression (19) for the conjugate scattering state. Namely, using the identity

$$\frac{1}{\varepsilon - H + i\rho} = \frac{1}{\varepsilon - H_{\rm sph} + i\rho} + \frac{1}{\varepsilon - H + i\rho}\times V_{\rm def}\frac{1}{\varepsilon - H_{\rm sph} + i\rho},$$

we transform it to the form

$$\langle\langle\alpha^{(-)}| = \langle\alpha^{(-)}| + \langle\langle\alpha^{(-)}|V_{\rm def}\frac{1}{\varepsilon - H_{\rm sph} + i\rho}. \quad (24)$$

Continuous spectrum solutions of the Shroedinger equation $H_{\rm sph}|\alpha^{(-)}\rangle = \varepsilon|\alpha^{(-)}\rangle$ together with the discrete spectrum solutions form a complete set of base states $\{|\alpha_{\rm cmpl}\rangle\} = \{|\alpha^{(-)}\rangle\}\cup\{|\alpha_{\rm disc}\rangle\}$. After multiplication of Eq. (24) on the right with the oscillator state $|N'l'j'm\rangle$ and using the completeness property of both the basis $\{|\alpha\rangle_{\rm cmpl}\}$ and oscillator states $|Nljm\rangle$ (in the limited space region of the interaction) we obtain

$$\langle\langle\alpha^{(-)}|N'l'j'm\rangle = \delta_{ll'}\delta_{jj'}\langle\varepsilon^{(-)}lj|N'l\rangle + \sum_{N''l''j''}\sum_{N_1'l_1'j_1'}\sum_{\tilde{\alpha}_{\rm cmpl}}\langle\langle\alpha^{(-)}|N''l''j''m\rangle\times\langle N''l''j''m|V_{\rm def}|N_1'l_1'j_1'm\rangle\langle N_1'l_1'j_1'm|\times\frac{1}{\varepsilon - H + i\rho}|\tilde{\alpha}_{\rm cmpl}\rangle\langle\tilde{\alpha}_{\rm cmpl}|N'l'j'm\rangle, \quad (25)$$

where $\langle\varepsilon^{(-)}lj|N'l\rangle = \int_0^\infty\langle\varepsilon^{(-)}lj|r\rangle\langle r|N'l\rangle r^2\,dr$ is the radial part of the scalar product $\langle\alpha^{(-)}|N'ljm\rangle$ and

$$\sum_{\tilde{\alpha}_{\rm cmpl}} \equiv \sum_{\tilde{l}\,\tilde{j}\,\tilde{m}}\left\{\int_{\tilde{\varepsilon}\geqslant 0} d\tilde{\varepsilon} + \sum_{{\rm Re}\tilde{\varepsilon}<0}\right\}.$$

We have

$$\sum_{\tilde{\alpha}_{\rm cmpl}}\langle N_1'l_1'j_1'm|\frac{1}{\varepsilon - H_{\rm sph} + i\rho}|\tilde{\alpha}_{\rm cmpl}\rangle\langle\tilde{\alpha}_{\rm cmpl}|N'l'j'm\rangle = \delta_{l'l_1'}\delta_{j'j_1'}\left\{\int_0^\infty\frac{\langle N_1'l'|\tilde{\varepsilon}^{(-)}l'j'\rangle\langle\tilde{\varepsilon}^{(-)}l'j'|N'l'\rangle\,d\tilde{\varepsilon}}{\varepsilon - \tilde{\varepsilon} + i\rho} + \sum_{{\rm Re}\tilde{\varepsilon}<0}\frac{\langle N_1'l'|\tilde{\varepsilon}l'j'\rangle\langle\tilde{\varepsilon}\,l'j'|N'l'\rangle}{\varepsilon - \tilde{\varepsilon}}\right\}. \quad (26)$$

The second term in this expression can be neglected since $|\varepsilon - \tilde{\varepsilon}|$ is large for discrete states in the region of the SDNP "resonance." The first term inside the curly braces can be expressed as

$$f_{N_1'N'l'j'}(\varepsilon) = P\int_0^\infty \frac{\langle N_1'l'|\varepsilon'^{(-)}l'j'\rangle\langle\varepsilon'^{(-)}l'j'|N'l'\rangle d\varepsilon'}{\varepsilon-\varepsilon'} - i\pi\langle N_1'l'|\varepsilon^{(-)}l'j'\rangle\langle\varepsilon^{(-)}l'j'|N'l'\rangle. \quad (27)$$

It follows from (26) and (27) that relationship (25) can be rewritten as a system of algebraic equations with respect to the $Nljm$ components of the scattering state $\langle\langle\alpha^{(-)}|$ in the region of interaction:

$$\sum_{N''l''j''} W_{N'l'j',\,N''l''j''}(\varepsilon,m)\langle\langle\alpha^{(-)}|N''l''j''m\rangle = -\delta_{ll'}\delta_{jj'}\langle\varepsilon^{(-)}lj|N'l\rangle, \quad (28)$$

where the elements of the W matrix are defined by the expression

$$W_{N'l'j',\,N''l''j''}(\varepsilon,m) = \sum_{N_1'} f_{N_1'N'l'j'}(\varepsilon)\langle N''l''j''m|V_{\rm def}|N'l'j'm\rangle - \delta_{N'N''}\delta_{l'l''}\delta_{j'j''}. \quad (29)$$

The number of significant components $\langle\langle\alpha^{(-)}|Nljm\rangle$ of the scattering state in the region of interaction, which determines the effective dimension of the W matrix at fixed values of the energy $\varepsilon = E_\gamma - B_{\rm thr}$ and angular moment projection $m = \nu + m_\beta$ [see (11)], is not very large due to the following:

(1) conservation of parity, $(-1)^l = (-1)^N = -(-1)^{N_\beta}$;
(2) the fact that the orbital momentum of the knocked out nucleon is limited by the constraint following from classical mechanics, $0 \leqslant l \lesssim l_{\max} = kR_{\rm react}$;
(3) additional conditions, $l \leqslant N \leqslant N_{\max}$, $|l - \frac{1}{2}| \leqslant j \leqslant l + \frac{1}{2}$, $j \geqslant |m|$ (where $N_{\max}$ can be chosen approximately equal to $l_{\max} + 4$, which allows one to describe correctly the $\langle\langle\alpha^{(-)}|Nljm\rangle$ components with large orbital momentum values).

Taking into account these limitations the optimal dimension of the system (29) does not exceed 100×100 at $E_\gamma \lesssim 50$ MeV.

IV. DEFORMED OPTICAL POTENTIAL

The spherical optical potential is of the form [28]

$$V_{\rm sph}(r) = -(V_1 + iW_1)\frac{1}{1+\exp[(r-R_1)/a_1]} - 4iW_2\frac{\exp[(r-R_2)/a_2]}{\{1+\exp[(r-R_2)/a_2]\}^2} - (V_3 + iW_3)\left(\frac{\hbar}{m_\pi c}\right)^2\frac{1}{2a_3 r} \times \frac{\exp[(r-R_3)/a_3]}{\{1+\exp[(r-R_3)/a_3]\}^2}\,\mathbf{s}\cdot\mathbf{l} + V_{\rm Coul}(r), \quad (30)$$

where the first two terms describe the nuclear forces, the third term corresponds to the spin-orbit interaction, and the fourth term

$$V_{\rm Coul}(r) = \begin{cases} \frac{3}{2}\frac{qZe^2}{R_{\rm Coul}}\left(1 - \frac{r^2}{3R_{\rm Coul}^2}\right) & \text{if } r \leqslant R_{\rm Coul}, \\ \frac{qZe^2}{r} & \text{if } r \geqslant R_{\rm Coul} \end{cases} \quad (31)$$

corresponds to the Coulomb interaction (q is 0 for a neutron, and 1 for a proton, $R_{\rm Coul} = r_{\rm Coul}A^{1/3}$ is the Coulomb radius).

If the nucleus is an oblate or prolate ellipsoid of revolution with the semiaxes c and d directed, respectively, along the nuclear symmetry axis and orthogonal to it, then its surface is described with the function

$$R(\theta) = R_0(1-\eta)^{1/6}(1-\eta\cos^2\theta)^{-1/2}, \quad (32)$$

where R_0 is the radius of the nondeformed nucleus ($R_0^3 = cd^2$), $\eta = (c^2 - d^2)/c^2$ is a deformation parameter connected with nuclear quadrupole deformation parameter $\delta = \frac{3}{2}(c^2 - d^2)/(c^2 + 2d^2)$ with the following relationship:

$$\eta = \frac{2\delta}{1 + 4\delta/3}. \quad (33)$$

The radial and angular dependencies of the nuclear component of the average field are in a close correlation with the distribution of nuclear matter density. If the thickness of the diffuse surface layer of the nucleus is small in comparison with its radius, then variation of this component of the average field due to deformation can be taken into account by introducing the angular dependence of R_1 and R_2 in (30) according to Eq. (32), where R_0 is substituted with R_1 and R_2, respectively.

Analogously to [32] the effect of deformation on the spin-orbit interaction is neglected, and for the Coulomb field that strongly affects proton scattering we use in the deformed optical potential $V(r,\theta)$ the expression obtained in [33]:

$$V_{\rm Coul}(r,\theta) = \begin{cases} \frac{3}{2}\frac{qZe^2}{R_{\rm Coul}}\Big[\Big(1 - \frac{r^2}{3R_{\rm Coul}^2}\Big) + \sum_{n=1}^{\infty}\Big(\alpha_n + \beta_n\frac{r^2}{R_{\rm Coul}^2}P_2(\cos\theta)\Big)\eta^n\Big] & \text{if } r \leqslant R(\theta), \\ qZe^2\Big[\frac{1}{r} + \sum_{n=1}^{\infty}\sum_{l=0}^{n}\gamma_{nl}\frac{R_{\rm Coul}^{2l}}{r^{2l+1}}P_{2l}(\cos\theta)\eta^n\Big] & \text{if } r > R(\theta), \end{cases} \quad (34)$$

where $R(\theta)$ is determined from (32) substituting $R_0 \to R_{\rm Coul}$ and the coefficients $\alpha_n, \beta_n, \gamma_{nl}$ are defined by the expressions

$$\alpha_n = \sum_{k=0}^{n} \frac{(-1)^k \Gamma_k(1/3)}{(2n-2k+1)k!}, \quad \beta_n = \frac{2}{(2n+1)(2n+3)},$$

$$\gamma_{nl} = \frac{3}{(2l+3)!!} \sum_{k=l}^{n} \frac{(-1)^{n-k}\Gamma_{n-k}\left(\frac{2l+3}{6}\right)(2l+2k+1)!!}{2^{2l+k}(n-k)!\,k!} \sum_{m=0}^{l} \frac{(-1)^m (4l-2m)!}{m!\,(2l-m)!\,(2l-2m)!\,(2l-2m+2k+1)}. \quad (35)$$

[Here $\Gamma_j(x) = x(x-1)\ldots(x-j+1)$ with $j = 1,2,\ldots$; $\Gamma_0(x) = 1$.]

The infinite series in (34) converge when $|\eta| < 1$, thus enabling description of the Coulomb component of the optical potential $V(r,\theta)$ for the quadrupole deformations $-0.3 < \delta < 1.5$. When $\delta \lesssim 0.4$ only the first ten elements of the series need to be considered.

From definition (12) the potential $V_{\rm def}(r,\theta)$ that was used in the previous section for derivation of the system of equations for coupled lj channels is given by the expression

$$V_{\rm def}(r,\theta) = V(r,\theta) - V_{\rm sph}(r). \quad (36)$$

It can be expanded into spherical harmonics

$$V_{\rm def}(r,\theta) = \sum_{\lambda} v_\lambda(r) Y_{\lambda 0}(\theta), \quad (37)$$

where λ takes the values $0,2,4,\ldots$ and the $v_\lambda(r)$ function is defined by the expression

$$v_\lambda(r) = 4\pi \int_0^1 V_{\rm def}(r,\theta) Y_{\lambda 0}(\theta)\, d(\cos\theta). \quad (38)$$

Using expansion (37) the matrix element $\langle N''l''j''m|V_{\rm def}|N'l'j'm\rangle$ from (29) can be rewritten in the form

$$\langle N''l''j''m|V_{\rm def}|N'l'j'm\rangle = \sum_{\lambda} \langle N''l''|v_\lambda(r)|N'l'\rangle \langle l''j''m|Y_{\lambda 0}(\theta)|l'j'm\rangle, \quad (39)$$

where the radial matrix element $\langle N''l''|v_\lambda(r)|N'l'\rangle$ is calculated numerically and calculation of the angular matrix element $\langle l''j''m|Y_{\lambda 0}(\theta)|l'j'm\rangle$ is performed according to (23).

V. (γ,p) REACTIONS ON ^{160}Gd, ^{184,186}W

The above described model was used to calculate cross sections of the proton SDNP in ^{160}Gd, ^{184,186}W for which experimental data obtained in a bremsstrahlung beam using the activation technique are available in the literature [34,35]. The calculation was performed in the energy range $E_\gamma = [0,60]$ MeV with variable energy step $h \leqslant 0.1$ MeV.

In order to compare the calculated SDNP cross sections with the experiment they have to be smeared over a certain energy interval Δ since the presented theoretical description does not take into account the fact that the ground state of a deformed final nucleus in laboratory the frame corresponds to a rotational band built upon it, so the energy of the outgoing nucleon is not exactly equal to $\varepsilon = E_\gamma - E_{\rm thr}$, and also in order to equalize the energy resolutions of measured and calculated data. The theoretical cross sections $\sigma(E_i), i = 1,2,\ldots$ were averaged over the energy interval $\Delta = 2$ MeV:

$$\bar\sigma(E) = \sum_i \frac{1}{2\pi} \frac{\Delta(E_{i+1} - E_i)}{(E_i - E)^2 + (\Delta/2)^2} \sigma(E_i). \quad (40)$$

Concerning other calculation details we note that the maximum value of the outgoing proton energy ε' in integral (27) was set to 50 MeV. Only spherical harmonics with $\lambda \leqslant 4$ were considered in the expansion of $V_{\rm def}(r,\theta)$ [see (37)]. The potential itself (as described in Sec. IV) was calculated using the spherical global optical potential from Ref. [28]. The scattering states in the spherical optical potential $V_{\rm sph}(r)$ were calculated using the program [36].

The statistical components of the photoproton cross section (compound and pre-equilibrium decay modes) were also taken into account. For their calculation the combined model of photonuclear reactions [37] with a standard parameter set was used. The quadrupole deformation parameters of ^{160}Gd and ^{184,186}W were estimated using the Stone static quadrupole moments compilation [38]. The main results of the calculations are shown in Figs. 2–4.

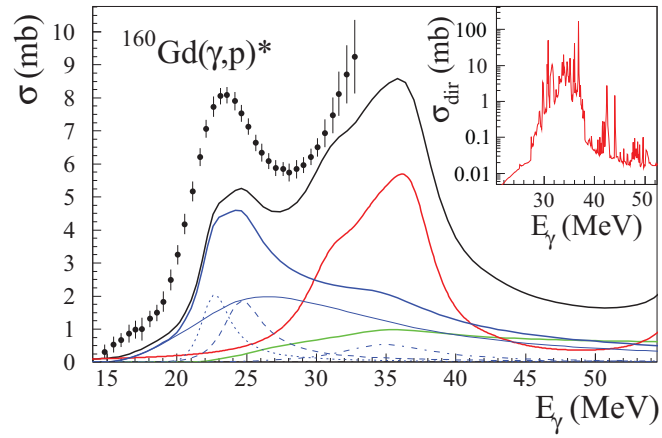

FIG. 2. Inset: calculated SDNP cross section of the (γ,p) reaction on ^{160}Gd without smearing; black circles with statistical errors: experimental cross section of the $(\gamma,p)^*$ reaction [35]; blue and green thick lines: cross sections of, respectively, the (γ,p) and (γ,np) reactions proceeding through decay of composite state calculated using the combined model [37]; red line: smeared SDNP cross section of (γ,p); black line: resulting theoretical estimate of the $(\gamma,p)^*$ cross section. Thin blue solid, dotted, dashed, dash-dotted curves show separate components of the decay cross section of (γ,p): respectively, the $T_<$ component of the GDR, the $T_>$ component, the isovector quadrupole resonance, the GDR overtone [37].

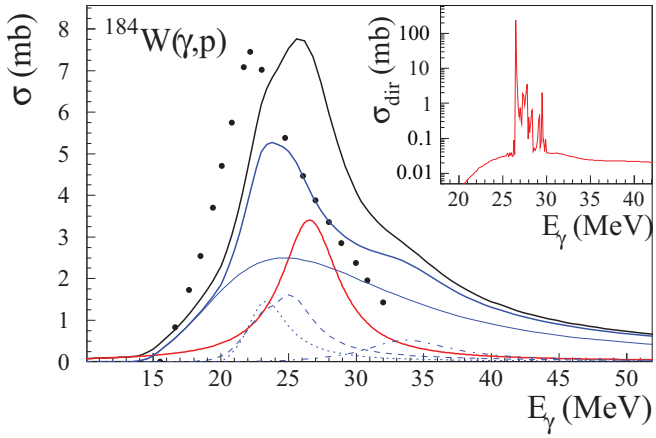

FIG. 3. Comparison of the experimental [34] and calculated cross sections of the (γ,p) reaction on ^{184}W. Same notation as in Fig. 2.

Figure 2 shows experimental [35] and theoretical cross sections of the $(\gamma,p)^* = (\gamma,p) + (\gamma,np)$ reaction on the ^{160}Gd nucleus. The inset shows the calculated SDNP cross section of the (γ,p) reaction in logarithmic scale without smearing. The main pane of the figure shows the experimental cross section of the $(\gamma,p)^*$ reaction [35] (black circles with statistical errors), the cross sections of the (γ,p) and (γ,np) reactions proceeding through decay of composite state calculated using the combined model [37] (respectively, blue and green thick lines), the smeared SDNP cross section of the (γ,p) reaction (red line), and the resulting theoretical estimate of the $(\gamma,p)^*$ reaction cross section obtained by summation of these curves (black line). In addition, thin blue curves show separate components of the decay cross section of (γ,p): the solid curve corresponds to the $T_<$ component of the GDR, the dotted curve to the $T_>$ component of the GDR, the dashed curve to the isovector quadrupole resonance, the dash-dotted curve to the GDR overtone [37].

It should be noted that the activation technique employed in [35] did not make it possible to separate the yields of reactions ^{160}Gd$(\gamma,p)^{159}$Eu and ^{160}Gd$(\gamma,np)^{158}$Eu and, therefore, only

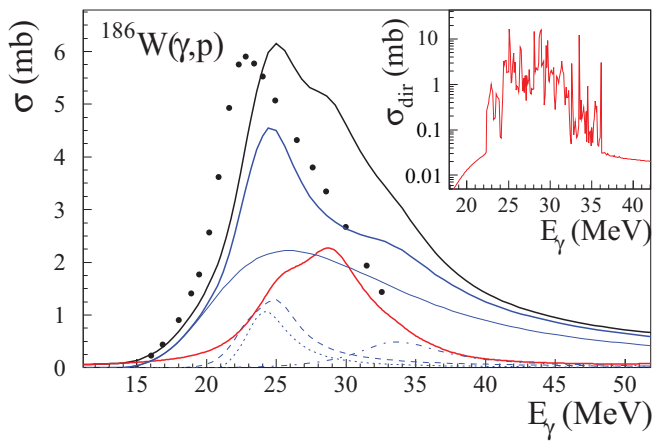

FIG. 4. Comparison of the experimental [34] and calculated cross sections of the (γ,p) reaction on ^{186}W. Same notation as in Fig. 2.

the sum of these cross sections was measured up to $E_\gamma = 32.7$ MeV. It is seen that the statistical model predicts that the (γ,p) cross section has to gradually decrease behind the maximum at $E_\gamma \approx 23$ MeV, since new channels of decay of the composite system open. However, the experiment shows that starting with the energy $E_\gamma \approx 28$ MeV there is a rather steep increase of the combined cross section of (γ,p) and (γ,np), which is attributed by the authors of work [35] to the contribution of the (γ,np) reaction. This interpretation is, however, probably incorrect, since due to the Coulomb barrier the decay of an excited composite system with emission of a neutron and a proton cannot compete with purely neutron emission channels [first of all with the $(\gamma,3n)$ reaction with the energy threshold of 21.3 MeV]. Indeed, a detailed calculation using the combined model [37] shows that the ^{160}Gd(γ,np) reaction cross section is comparatively small (green curve in Fig. 2). This suggests that the (γ,p) reaction cross section contains a significant contribution of the direct photoeffect which is manifested at $E_\gamma > 28$ MeV.

With the SDNP model described in this work only the target nucleus deformation and the single-particle state $|\beta\rangle$ which the nucleon is knocked out from have to be specified as input data. The quadrupole deformation of the ^{160}Gd nucleus is $\delta \approx 0.33$. For this nucleus the last occupied state in deformed single-particle potential from which the proton is knocked out corresponds to the orbital with asymptotic quantum numbers $[N = 4, n_z = 1, \Lambda = 3, \Omega = 5/2]$, where N is the total number of oscillator quanta, n_z is their number along the nuclear symmetry axis, Λ and Ω are the projections of the orbital and total angular momenta on the symmetry axis [39]. This assignment is in good agreement with the $J^\pi = \frac{5}{2}^+$ ground state of the final nucleus ^{159}Eu. As it is seen from Fig. 2, with such choice of the deformation and the $|\beta\rangle$ state the calculated cross section of the SDNP (γ,p) reaction (shown with red curve) apparently correlates with the experimental data.

It also follows from Fig. 2 that the broad maximum observed in the experimental (γ,p) reaction cross section at $E_\gamma \approx 23$ MeV can hardly be attributed to the giant quadrupole resonance, which accounts only for a relatively small fraction of the peak area.

It should be mentioned that in comparison of theoretical and experimental cross sections one has to take into account large systematic errors that necessarily arise during estimation of the statistical reaction component of (γ,p) at $E_\gamma \sim 30$ MeV, since the detailed behavior of the GDR far from the photoabsorption peak is mostly unknown. The GDR strength function of deformed nuclei is usually approximated with two Lorentz curves. However, this leads to interference of the parameters of these Lorentz curves. If, for example, the width parameter Γ of the second, higher energy Lorentz curve is increased, this results in enlargement of the high energy tail of the GDR. The total cross section of the (γ,p) reaction also grows appropriately, becoming more compatible with the experimental data. The systematic errors of the activation technique measurement itself that can easily be large have also to be taken into consideration.

The theoretical and experimental [34] cross sections of the (γ,p) reaction on ^{184}W are compared in Fig. 3. The notation is

the same as in Fig. 2, except for not showing the (γ,np) reaction cross section which had not been measured in the experiment.

The quadrupole deformation parameter δ of the ^{184}W nucleus is 0.24. The ground state of the final nucleus ^{183}Ta has $J^\pi = \frac{7}{2}^+$, implying that the last filled proton state ($|\beta\rangle$) of the ^{184}W nucleus corresponds to an orbital with asymptotic quantum numbers $[N = 4, n_z = 0, \Lambda = 4, \Omega = 7/2]$ in the single-particle deformed potential. It is seen from the figure that the magnitude of the experimental cross section is properly reproduced by the calculation but the peak of the theoretical cross section is shifted by about 3 MeV towards higher energies in comparison with the experimental cross section. One can also see that the SDNP contribution to the total cross section is substantial, but not as large as in the case of ^{160}Gd.

Figure 4 shows similar data for the ^{186}W nucleus. The deformation parameter of ^{186}W is $\delta = 0.20$. As δ changes from 0.24 to 0.20 the proton orbital $[4\,0\,4\,\frac{7}{2}]$ in the deformed single-particle potential descends below the $[4\,1\,1\,\frac{1}{2}]$ proton orbital, and, therefore, the latter has been chosen as the $|\beta\rangle$ state for ^{186}W. As it is seen from the figure the agreement with the experiment is somewhat better for this isotope than in the case of ^{184}W, though a certain shift of the peak of the theoretical cross section is also visible. As with ^{160}Gd and ^{184}W the SDNP contribution (red curve) leads to a significant increase of photoproton yield in the considered energy range.

The observed difference of the widths of the calculated SDNP "resonances" of the ^{160}Gd and ^{184,186}W nuclei can be explained by the difference of the initial nucleon configurations $|\beta\rangle$. The least broad resonance corresponds to the ^{184}W nucleus, where the $|\beta\rangle$ state is practically identical to the $|N = 4, l = 4, j = \frac{7}{2}, \Omega = \frac{7}{2}\rangle$ spherical oscillator state. The situation is different for the two other nuclei: the $|\beta\rangle$ state contains several different orbital l and angular j momentum values.

It also follows from the performed calculations that the angular distribution of the SDNP protons for the considered nuclei is close to isotropic with $|A_2/A_0| < 0.03$ [see Eq. (8)].

VI. CONCLUSIONS

The SDNP reaction mechanism considered in this work has a significant effect on the photoproton yield from heavy deformed nuclei in the energy range $E_\gamma \sim 30$ MeV. Unfortunately, no recent measurements of the (γ, p) reaction on heavy deformed nuclei at these energies could be found in the literature, so the experimental results obtained in the 1960s–1970s were used for comparison. However, the performed analysis clearly shows the relevance of the considered approach and the necessity of further experimental and theoretical research in this direction for both deformed and spherical nuclei.

The following results were obtained in the present work:

(1) A model of SDNP for heavy deformed nuclei, for which to the first order of approximation nuclear surface vibrations can be neglected, is formulated within the adiabatic approach.
(2) A compact system of algebraic equations for the coupled lj reaction channels was obtained, which allows the problem of calculation of scattering states at $r \lesssim R_{\text{peak}}$ in deformed average field to be reduced to calculations in a spherical average field.
(3) The SDNP contribution to the (γ, p) reaction cross sections was calculated for the ^{160}Gd and ^{184,186}W nuclei. Comparison of the calculated and experimental data shows importance of the SDNP effect at least for the proton reaction channel at the high-energy tail of the GDR (at $E_\gamma \sim 30$ MeV).
(4) The calculated angular distribution of the SDNP protons was almost isotropic for the considered nuclei ($|A_2/A_0| < 0.03$ in the region of the obtained proton bump).

Is should be noted that the correlation between the experimental and theoretical data is achieved using the global optical potential [28] to describe the spherical average nuclear field, whose parameters are adjusted independently of the considered effect, from nucleon scattering data. The comparison of experimental and theoretical results also reveals the important role of $E1$ photoabsorption in formation of the SDNP "resonances" in heavy deformed nuclei.

Among the distinctive features that distinguish the SDNP from other mechanisms of nuclear photoeffect one can name the high energy of the SDNP "resonance" and the energy distribution of the outgoing nucleons which has the form of a narrow peak at the energy $\varepsilon_0 = E_\gamma - B_{\text{thr}}$.

[1] C. Cline and M. Blann, Nucl. Phys. A **172**, 225 (1971).
[2] C. Kalbach-Cline, Nucl. Phys. A **210**, 590 (1973).
[3] E. Gadioli, E. Erba, and P. Sona, Nucl. Phys. A **217**, 589 (1973).
[4] J. Dobeš and E. Běták, Nucl. Phys. A **272**, 353 (1976).
[5] M. Blann, Phys. Rev. Lett. **27**, 337 (1971).
[6] M. Blann, Phys. Rev. Lett. **28**, 757 (1972).
[7] M. Blann and H. K. Vonach, Phys. Rev. C **28**, 1475 (1983).
[8] H. Feshbach, A. Kerman, and S. Koonin, Ann. Phys. **125**, 429 (1980).
[9] T. Tamura, T. Udagawa, and H. Lenske, Phys. Rev. C **26**, 379 (1982).
[10] H. Nishioka, J. Verbaarschot, H. Weidenmller, and S. Yoshida, Ann. Phys. **172**, 67 (1986).
[11] H. Nishioka, H. Weidenmller, and S. Yoshida, Ann. Phys. **183**, 166 (1988).
[12] J. Akkermans and A. Koning, Phys. Lett. B **234**, 417 (1990).
[13] A. Koning and J. Akkermans, Ann. Phys. **208**, 216 (1991).
[14] A. J. Koning and M. B. Chadwick, Phys. Rev. C **56**, 970 (1997).
[15] T. Tamae, T. Hino, H. Kawahara, M. Nomura, M. Sugawara, A. Tanaka, T. Tanaka, H. Tsubota, T. Yokokawa, and T. K. Yoshida, Nucl. Phys. A **690**, 355 (2001).
[16] D. Wilkinson, Physica **22**, 1039 (1956).
[17] C. Bloch, Nucl. Phys. **4**, 503 (1957).
[18] J. S. Levinger, *Nuclear Photo-disintegration* (Oxford University Press, New York, 1960).

[19] F. S. Dietrich, D. W. Heikkinen, K. A. Snover, and K. Ebisawa, Phys. Rev. Lett. **38**, 156 (1977).
[20] A. Likar, F. Sever, and R. Martinčič, Nucl. Phys. A **307**, 77 (1978).
[21] A. Likar and T. Vidmar, Nucl. Phys. A **593**, 69 (1995).
[22] A. Likar and T. Vidmar, Nucl. Phys. A **611**, 56 (1996).
[23] S. Boffi, C. Giusti, and F. Pacati, Nucl. Phys. A **359**, 91 (1981).
[24] J. T. Londergan and L. D. Ludeking, Phys. Rev. C **25**, 1722 (1982).
[25] G. Lotz and H. Sherif, Nucl. Phys. A **537**, 285 (1992).
[26] A. Bohr and B. Mottelson, *Nuclear Structure* (World Scientific, Singapore, New Jersey, 1998), Vol. 1.
[27] A. G. Sitenko and V. K. Tartakovsky, *Lectures on the Theory of the Nucleus* (Pergamon, Oxford, 1975).
[28] A. J. Koning and J. P. Delaroche, Nucl. Phys. A **713**, 231 (2003).
[29] F. Villars, in *Fundamentals in Nuclear Theory*, edited by A. de-Shalit and C. Villi (IAEA, Vienna, Austria, 1967), p. 269.
[30] S. G. Nilsson, Kong. Dan. Vid. Sel. Mat. Fys. Med. **29**, 1 (1955).
[31] C. Gustafson, I. L. Lamm, B. Nilsson, and S. G. Nilsson, Ark. Fys. **36**, 613 (1967).
[32] T. Tamura, Rev. Mod. Phys. **37**, 679 (1965).
[33] B. S. Ishkhanov and V. N. Orlin, Phys. At. Nucl. **68**, 1352 (2005).
[34] J. H. Carver, D. C. Peaslee, and R. B. Taylor, Phys. Rev. **127**, 2198 (1962).
[35] F. Dreyer, H. Dahmen, J. Staude, and H. Thies, Nucl. Phys. A **192**, 433 (1972).
[36] W. R. Smith, Comput. Phys. Commun. **1**, 106 (1969).
[37] B. S. Ishkhanov and V. N. Orlin, Phys. At. Nucl. **78**, 557 (2015).
[38] N. Stone, At. Data Nucl. Data Tables **90**, 75 (2005).
[39] A. Bohr and B. R. Mottelson, *Nuclear Structure* (World Scientific, Singapore, New Jersey, 1998), Vol. 2.